Journal of Fluorescence, Vol. 8, No. 1, 1998

Fluorescence Resonance Energy Transfer: FRET Studies of Ligand Binding to Cell Surface Receptors

Angelique Y. Louie[1,2,4] and Bruce J. Tromberg[2,3,5]

Received May 14, 1997; accepted January 28, 1998

We describe a simple optical system employing fluorescence resonance energy transfer (FRET) to identify potential binding domains on the macrophage scavenger receptor for the ligand maleylated bovine serum albumin (mal-BSA). Using a plasma membrane vesicle system, we placed donor probes on the ligand and acceptor probes in the membrane to determine the distance of bound ligand from the cell surface. Two donors and three acceptors were employed. Transfer between ligand covalently modified with multiple dansyl molecules and hexadecanoylaminoeosin in the membrane yielded a distance of 46.5 ± 7.5 Å; transfer from the same type of donors to octadecylrhodamine B in the membrane gave a distance of 58.5 ± 3.0 Å. No transfer was observed between ligand mono-labeled with fluorescein and 1,1'-dioctadecyl-3,3,3',3'-tetramethylindocarbocyanineperchlorate in the membrane. This suggests that the orientation of mal-BSA bound to the receptor places the fluorescein probe too far from the lipid surface to experience energy transfer. The distance information identifies a potential location for the binding site, which can be compared to structural information about the receptor and used to extract a binding sequence.

KEY WORDS: Transmembrane protein; binding site; resonance energy transfer; intramolecular distances; modified low-density lipoprotein (LDL) receptor.

INTRODUCTION

Transport of materials into cells can occur by passive diffusion or by receptor-mediated or nonspecific endocytosis. The interactions of drugs in the treatment of disease often involves blocking the uptake or binding of ligands by particular receptors. Alternatively, specific receptors can be exploited as a means for delivering drugs to particular cells. Detailed knowledge of the nature and structure of the binding site on a receptor aids in the design of agents to interfere or interact with receptor function.

Identification of binding sites on receptor proteins typically involves the generation of truncation or site specific mutants. However, the results from binding studies with such mutants can be ambiguous; for instance, deletion of a region which is key to structural integrity can abolish function but the region may not be directly involved with binding. Furthermore, these types of studies may supply primary sequence information regarding the binding site but give no insight to the location of the binding site in the overall protein structure. Alternatives to molecular techniques include optical technologies such as fluorescence resonance energy transfer (FRET) and more sophisticated methods including nuclear magnetic resonance (NMR) and x-ray crys-

[1] Department of Developmental and Cell Biology, University of California, Irvine, California 92612.
[2] Beckman Laser Institute and Medical Clinic, University of California, Irvine, California 92612.
[3] Department of Physiology and Biophysics, University of California, Irvine, California 92612.
[4] Present address: Mail code 139-74, California Institute of Technology, Pasadena, California 91125.
[5] To whom correspondence should be addressed at Beckman Laser Institute, 1002 Health Sciences Road East, Irvine, California 92612-1475. e-mail: tromberg@nova.bli.uci.edu

1053-0509/98/0300-0013$15.00/0

tallography. FRET offers the advantage of being able to study the binding characteristics of an unmanipulated receptor *in situ* while providing some degree of structural information.

Detailed structural information can be derived from x-ray crystallography, however, few transmembrane proteins have been successfully prepared for such studies. The transmembrane domain makes it more difficult to purify such proteins and removal from the membrane can perturb the structure of the protein. NMR is an alternative means for obtaining structural information, but it is limited largely to molecules less than 30 kD in size and requires relatively large amounts of purified material for study (millimoles of protein). While FRET does not yield information at the level of resolution of the aforementioned techniques, it is well suited to the study of transmembrane receptors in their native state.

FRET has long been utilized as a technique for measuring inter- and intramolecular distances. These measurements allow determination of such widely varying properties as substrate turnover rate in catalysis, molecular conformation changes, molecular aggregation/complexation, and three-dimensional structure. The characterization of membrane receptors by use of FRET between fluorescently labeled ligands and the membrane surface has been employed most extensively for the IgE receptor [4,5,20,21,38] and the nicotinic acetylcholine receptor [23,24,35,36] to probe the conformations of these receptors with bound ligands. Although the studies in the literature, for the most part, provide sufficient experimental detail on the collection of data, it is not always clear how these data are translated to a distance measurement from theory.

There are a number of solutions to the Forster energy transfer problem presented in the literature. Some of these are analytical solutions based on approximations made with regard to specific cases [10,14,37]; another approach is to obtain an exact solution by numerical methods such as described by Snyder and Freire. All of these solutions have been employed by various researchers to calculate distances from experimental data. A search of the literature can be confusing to investigators who wish to employ FRET for their own studies given this mix of analytical treatments.

We describe herein a simple optical technique, based on FRET, for studying receptor binding sites. The technique is described in simple terms and in sufficient detail for others to use these methods and utilizes, in a comprehensive manner, the key analytical points from past papers. We provide the conceptual framework and experimental approach to perform FRET in membrane systems and clearly outline the mathematical treatment of the data to obtain a distance measurement. The example system employed in these studies is the macrophage scavenger receptor, but the techniques described are readily extendable to characterize other transmembrane receptors in situ without perturbing their structure.

The class A macrophage scavenger receptor is a trimeric, transmembrane glycoprotein bearing an unusually broad ligand binding specificity, recognizing certain polypurines (polyinosinic, polyguanylic), modified albumins (malondialdehyde-modified, maleylated), modified low-density lipoproteins (LDL) (oxidized, acetylated), and some other negatively charged molecules [6]. The scavenger receptor is proposed to be a rigid stalk extending some 400 Å above the membrane surface and is believed to play a key role in cholesterol accumulation during the formation of foam cells, one of the early lipid deposition events in atherosclerosis [15,34].

For these studies we placed fluorescent donors on a scavenger receptor ligand, maleylated bovine serum albumin (mal-BSA), and assessed the distance of the bound ligand from the plasma membrane surface using various membrane-localizing acceptors.

MATERIALS AND METHODS

Materials. The fluorescent probes dansyl chloride, fluorescein maleimide, DiI (1,1'-dioctadecyl-3,3,3',3'-tetramethylindocarbocyanine perchlorate), HAE (hexadecanoylaminoeosin), and ORB (octadecylrhodamine B) were from Molecular Probes (Eugene, OR). Phosphatidylethanolamine (diluted 8:0) was from Avanti Polar Lipids, Inc. (Alabaster, AL). Thin-layer chromatography (TLC) plates and chloroform were from EM Science (Gibbstown, NJ), TEA (triethylamine) and BCA protein assay reagents were from Pierce Biochemicals (Rockford, IL). Ethyl acetate was from Fischer Scientific (Pittsburgh, PA). Maleic anhydride, *N*-ethylmaleimide (NEM), DNase I, bovine serum albumin, and all common shelf reagents were from Sigma (St. Louis, MO). RPMI 1640 medium, fetal bovine serum (FBS), penstrep, and L-glutamine were from GIBCO (Gaithersburg, MD). The P388D1 cell line was from the ATCC (Rockville, MD).

Maleylation of BSA [7]. Ninety-two milligrams of solid maleic anhydride was added in small aliquots with stirring to 10 ml of 10 mg/ml BSA in phosphate-buffered saline (PBS). The solution was maintained at pH 8.5–9.0 with 1 *N* NaOH or by the addition of solid sodium carbonate. After completion of the reaction, as indicated by stabilization of the pH, the solution was dialyzed in PBS, pH 7.4, by four changes.

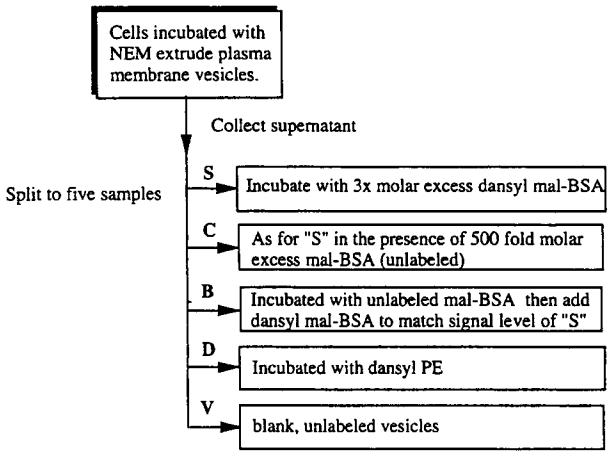

Fig. 1. Sample compositions. Sample preparation methods are outlined for the five samples employed to calculate the corrected donor emissions used in distance calculations: S (sample), C (nonspecific binding control), B (control for direct interaction between donor and acceptor), D (sample for determination of acceptor density), and V (blank). For more detail refer to Materials and Methods.

Fluorescent Labeling of Mal-BSA with Dansyl Chloride [30]. Dansyl chloride (5-dimethylaminonaphthalene-1-sulfonyl chloride, 20 m*M* in acetone) was added to mal-BSA in PBS at pH 8.0 to give a final weight ratio of 100:2. The mixture was incubated for 6 h at 4°C. Conjugates were separated from unreacted probes by gel filtration on a Sephadex G-25 column equilibrated with PBS, pH 7.4. Degree of substitution was determined spectrophotometrically using an extinction coefficient of 4500 M^{-1} cm^{-1} at 340 nm for dansyl amine conjugates [19]. Typical labeling placed 4–7 dansyl molecules per mal-BSA. Protein concentrations were determined by the BCA protein assay [29].

Maleylation and Fluorescein Labeling of BSA. BSA in PBS, pH 7.4, was incubated with a 50% molar excess of fluorescein maleimide (1 mg/ml in DMF) at room temperature for 1 h. The pH was then adjusted to 8.5 and the steps for maleylation were carried out as described above. The product was dialyzed in PBS, pH 7.4, against three changes. The protein concentration of the final product was determined by BCA assay and the degree of labeling determined spectrophotometrically using an extinction coefficient of 7.08×10^4 M^{-1} cm^{-1} for fluorescenyl maleimide groups at 495 nm [19].

Fluorescent Labeling of Phosphatidylethanolamine. 5-Dimethylaminonaphthalene-sulfonyl phosphatidylethanolamine (dansyl PE) was synthesized by reacting 5 mg of dansyl chloride with 200 µl of 25 mg/ml PE (diluted 8:0 in chloroform) and 100 µl of TEA. The reaction was monitored by silica gel TLC developed using an acidic developing solvent ($CHCl_3$–acetone–MeOH–acetic acid–H_2O, 50:20:10:10:5). When the reaction was complete the solvent was removed under nitrogen. Following ethyl acetate–acetone extraction the solid lipid material was redissolved in 95:5 $CHCl_3$:MeOH and applied to 20 × 20 silica gel preparative TLC plates. The plates were developed at room temperature in an acidic solvent system. Unreacted dansyl chloride ran as a nonfluorescent (UV excitation), yellow band at the solvent front. A fluorescent, brown band of unknown content trailed behind this yellow band. Dansyl PE migrated as a broad, yellow, fluorescent (UV excitation) band following the brown band. After development, the major band was scraped off and eluted from the gel with $CHCl_3$–MeOH–0.2 *N* HCl, 1:2:0.8. Dansyl PE was then extracted to chloroform/methanol by the method of Bligh-Dyer as modified by Longmuir *et al.* [27].

Cell Culture and Membrane Vesicle Preparation. P388D1 mouse monocyte–macrophages were maintained in RPMI 1640, 10% FBS and subcultured by scraping. Each experiment utilized 12 T225 flasks (Costar), yielding about 10^9 cells. The isolation of plasma membranes was performed as described previously [20]. Twenty-four hours prior to treatment the growth medium was removed and replaced with RPMI 1640, 10% lipoprotein-deficient serum in order to maximize the number of receptors expressed on the cell surface. Lipoprotein deficient serum was prepared as described by Robertson [31]. Prepared vesicles were stored at 4°C and used within 1 week. Vesicles were distributed to five samples as illustrated in Fig. 1. Sample S was incubated with dansyl mal-BSA in a 3-fold excess over the estimated 3×10^{-10} mol of receptors per sample; sample C was incubated with unlabeled mal-BSA in a 500-fold excess and dansyl mal-BSA (3-fold excess); sample D was incubated with 0.85 to 1.7 nmol dansyl-PE; sample B was incubated with unlabeled mal-BSA in a 500-fold excess; and one sample, V, was left untreated. All samples were brought to the same volume with PBS. After 4 h at room temperature or overnight at 4°C with stirring, the samples were diluted with PBS and centrifuged at 25,000*g* for 45 min at 4°C. The resulting pellets were resuspended in PBS/azide buffer (10 m*M* sodium phosphate, 0.15 *M* NaCl, 0.01% Na azide) or PBS/azide + 10% EtOH through a 25-gauge needle. Following resuspension free dansyl mal-BSA was added to sample B to match the fluorescence intensity of sample S.

Spectroscopy. Absorption spectra were recorded with a Beckman DU-7 spectrophotometer. Fluorescence measurements were conducted at room temperature with

an SLM 48000 spectrofluorometer (SLM-Aminco Inc., Urbana, IL). Acceptor was titrated into the vesicle samples and the fluoresence spectra were measured 1 h after each titration. Control samples were employed as follows: C was used to correct for contributions from nonspecific binding of donor and from acceptor fluoresence or vesicular autofluoresence; D was used to determine surface density, described later; dansyl mal-BSA was added to B to bring its peak fluoresence to the same intensity as S and was used to determine quenching of donor probe due to direct interaction of donor and acceptor; and V was used to correct for acceptor contributions or autofluoresence in sample D. Relative quantum yield changes were calculated from

$$Q_d = \frac{I_S - I_C}{I_B - I_C} \tag{1}$$

where Q_d is the quantum yield of the donor and I_S, I_B, and I_C are the emission intensities of the the respective samples at 510 nm [20]. Using Eq. (1), quantum yield of the donor was determined before the addition of acceptor (Q_d) and at each titration point (Q_{da}).

The density of the acceptor in the membrane plane was determined using D, which contained dansyl-PE as the donor in the same plane as the acceptor, and V. The acceptor concentration in the membrane was calculated from

$$\frac{Q_{da}}{Q_d} = \frac{I_D - I_V}{I_{oD} - I_{oV}} \tag{2}$$

where I_D, I_V, I_{0D}, and I_{0V} are the intensities of the samples in the presence and absence of acceptor and

$$\frac{Q_{da}}{Q_d} = 0.6463 \exp(-4.7497c) + 0.3537 \exp(-2.0618c) \tag{3}$$

where c is the surface density of acceptor per R_0^2 for a distance of closest approach between donor and acceptor equal to 0.0. The assumption was made that since both donor and acceptor lie in the membrane, the distance of closest approach goes to zero. In this case the expression for relative quantum yield can be approximated as given in Eq. 3 [37]. R_0 is the critical transfer distance at which one-half the donor decay is due to energy transfer. Values of Q_{da}/Q_d from Eq. (2) at each titration of acceptor were applied to Eq. (3) to find the corresponding c. In this manner, c could be determined for each molar concentration of acceptor added.

The quantum yield of the donor was obtained by the comparison method using the standard quinine sulfate. Given that quinine sulfate in 0.1 N H_2SO_4 at 350-nm excitation has $Q = 0.7$ at 23°C and that fluorescein in 0.1 N NaOH at 355-nm excitation has $Q = 0.93$ at 20°C, the quantum yield of the donor is calculated from

$$\frac{Q_1}{Q_2} = \frac{F_1}{F_2}\frac{A_2}{A_1} \tag{4}$$

where Q_n = is the quantum yield of sample n, F_n = is the area under the fluoresence emission curve for sample n, and A_n = is the absorption at the excitation wavelength for sample n [8].

Data Analysis. The Forster distance, R_0, was determined from [22]

$$R_o^6 = 8.79 \times 10^{-5} J\kappa^2 Q_D n^{-4} \text{Å}^6 \tag{5}$$

The spectral overlap integral between D and A is given by J

$$J = \frac{\int f_D(\lambda)\varepsilon_A(\lambda)\lambda^4}{\int f_D(\lambda)} d\lambda \qquad (\lambda \text{ in nm}) \tag{6}$$

where $f_D(\lambda)$ is the corrected emission of the donor and $\varepsilon_A(\lambda)$ is the extinction coefficient of the acceptor. The orientation factor for randomly oriented donors and acceptors is given by

$$\kappa^2 = 2/3$$

[9,24] and $n = 1.4$ is the index of refraction of the medium through which energy propogates [20].

From Eq. (1) and the surface density values generated by Eqs. (2) and (3), a plot of Q_{da}/Q_d versus c could be generated. Such a curve can be fitted by a single exponential of the form

$$\frac{Q_{da}}{Q_d} = \exp(-kc) \tag{7}$$

where k is a third-order polynomial as follows:

$$k = B(R_o/L) = \sum_{i=0}^{3} \alpha_i (R_o/L)^{-i} \tag{8}$$

where L is the distance of closest approach between donor and acceptor. The parameters $\alpha_0 = -3.448$, $\alpha_1 = -0.4021$, $\alpha_2 = 4.136$, and $\alpha_3 = -1.668$ were derived by numerical methods [33]. B is a constant. Curves of Q_{da}/Q_d versus c were fit to a single exponential and the value obtained for k was substituted into Eq. (8), which was iteratively solved for R_0/L. A plot of $y = \sum_{i=0}^{3} \alpha_i (R_0/L)^{-i}$ was used to make an initial guess for values of R_0/L that produce a y value equal to the determined k.

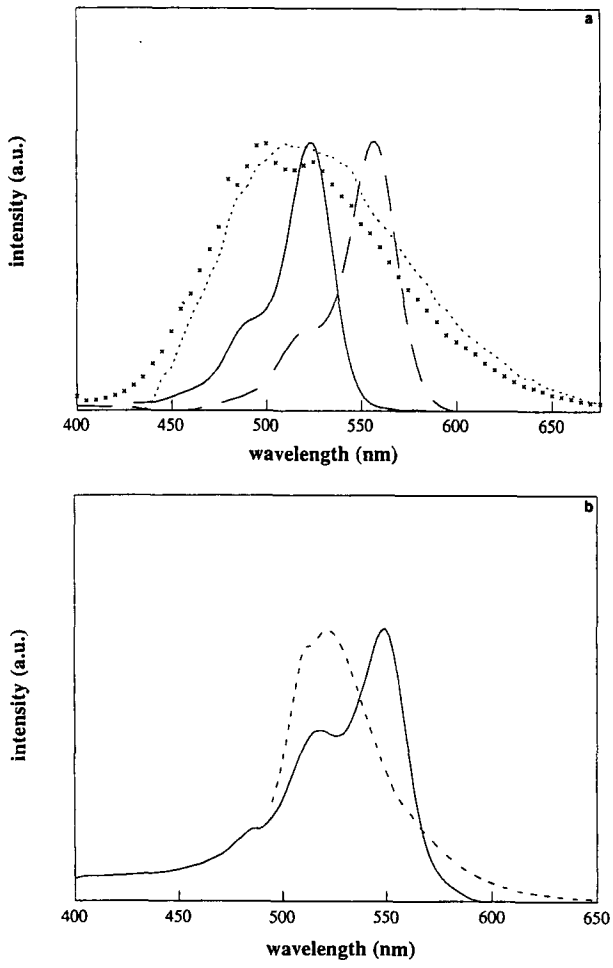

Fig. 2. Spectral overlap of donor and acceptor probes. (a) Corrected fluorescence emission spectra for dansyl mal-BSA in PBS (- - -), and 10% EtOH/PBS (xxx), excitation at 342 nm, and the absorption spectra for HAE (——) and ORB (——) in plasma membrane vesicles. (b) Fluorescence emission spectrum for fluorescein mal-BSA in PBS (– – –), excitation at 470 nm, and absorption spectra for DiI (——). Intensities are given as arbitrary units (a.u.).

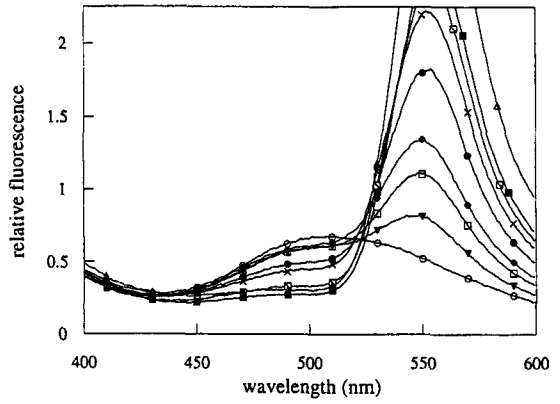

Fig. 3. Decrease in donor fluorescence intensity and corresponding enhancement of acceptor fluorescence intensity. The relative fluorescence intensities are shown for a representative experiment with the dansyl–HAE pair. As acceptor is added there is a decrease in donor fluorescence intensity and a corresponding increase in acceptor fluorescence intensity. Curves shown are corrected against a control for nonspecifically bound dansyl mal-BSA.

RESULTS

Spectral Overlap of Donor and Acceptor Probes. Spectra for the emission of dansyl probes on maleylated-BSA bound to NEM vesicles and absorption of HAE and ORB in vesicles are given in Fig. 2a. Spectra for the emission of fluorescein-labeled mal-BSA and absorption of DiI in NEM vesicles are presented in Fig. 2b. The emission peak for dansyl is slightly blue-shifted in 10% EtOH/PBS compared to the peak in PBS alone. Transfer experiments involving the dansyl–ORB pair were conducted in PBS/azide buffer containing 10% ethanol in order to facilitate acceptor insertion into the membrane. Data for changes in relative quantum yield of the donor upon addition of acceptor were collected at 520 nm for both buffer systems, with excitation at 342 nm for dansyl and 470 nm for fluorescein. Absorption maxima for DiI, HAE, and ORB occurred at 550, 525, and 555 nm, respectively.

Spectral Parameters. Quantum yield measurements resulted in values of 0.71 for dansyl-labeled mal-BSA in PBS, 0.297 for dansyl-labeled mal-BSA in 10% EtOH/PBS, and 0.104 for fluorescein-labeled mal-BSA. These spectral parameters yield Forster distances of 51.1 Å for the dansyl–HAE pair, 46.4 Å for the dansyl–ORB pair, and 44.7 Å for the fluorescein–DiI pair.

Energy Transfer Measurements. The change in donor quantum yield as acceptor inserts into the membrane is depicted in Figs. 3 and 4 for a representative experiment with the dansyl–HAE pair. Figure 3 demonstrates that the enhancement of acceptor fluorescence intensity follows exactly the decrease in donor fluorescence intensity, which indicates that energy transfer is occurring. In addition, there is no change to the acceptor and donor profiles other than intensity, implying that they are the same species, which again supports that energy transfer is occurring as opposed to a species modifying event such as charge transfer. In Fig. 4 the concentration of acceptor is given in terms of surface density, calculated as described under Materials and Methods. This plot of Q_{da}/Q_d versus surface density could be fit by the exponential function predicted for energy transfer: $\exp(-kC)$, where k was determined to be 1.237. Applying Eqs. (7) and (8), this corresponds to a distance of closest approach of 41.3 Å between donor and acceptor. Five in-

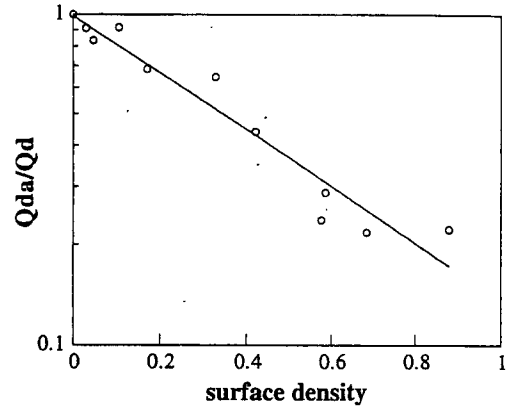

Fig. 4. Energy transfer between receptor-bound dansyl mal-BSA and acceptors at the membrane surface. The ratio of donor quantum yield in the absence (Q_d) and presence (Q_{da}) of acceptor HAE is plotted as a function of the surface density of the acceptor (acceptors/R_0^2). Semilog plot from a representative experiment (five separate trials performed) shows the best exponential fit of the data.

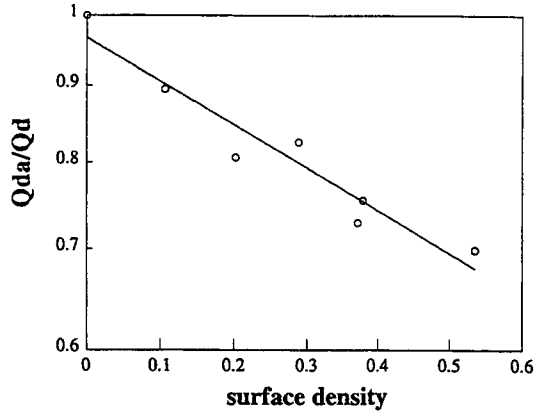

Fig. 5. Energy transfer between receptor-bound dansyl mal-BSA and acceptors at the membrane surface. The ratio of donor quantum yield in the absence (Q_d) and presence (Q_{da}) of acceptor ORB is plotted as a function of the surface density of the acceptor (acceptors/R_0^2). Semilog plot from a representative experiment (seven separate trials performed) shows the best exponential fit of the data.

dependent repeats of these measurements resulted in an average distance of 46.5 ± 7.5 Å (SD). These experiments were repeated with a second amphipathic acceptor, ORB. In order to facilitate the partitioning of ORB into the membrane bilayer, ethanol was added to the vesicle suspensions to a final concentration of 10%. Data from a single experiment with the dansyl–ORB pair is given in Fig. 5. This plot could be fit to Eq. (7) with a decay constant of 0.782, which from Eq. (8), gives a distance value of 59.34 Å. Data averaged over seven independent experiments gave a distance of 58.5 ± 3.0 Å.

Experiments conducted with fluorescein–DiI show no evidence of energy transfer between donor and acceptor. No change of donor quantum yield was observed upon the addition of the acceptor. To verify that the acceptor partitioned into the membrane bilayer, the enhancement of DiI fluorescence as the probe associated with this hydrophobic environment was monitored over time. DiI was introduced to a solution of membrane vesicles and its fluorescence at 575 nm (excitation, 530 nm) monitored at 5-min intervals. Probe association with the hydrophobic environment of the lipid bilayer was demonstrated by a 30% increase in relative fluorescence over time, which plateaued after 60 min.

DISCUSSION

In order to estimate receptor binding site distance from the surface of intact plasma membranes, we have considered the fluorescent donor to be a rigid point source residing at a fixed location above a semiinfinite planar surface. This simplification is not unreasonable due to the fact that the receptor is shown to have a rigid stalk structure and the binding domain is likely to be small and in close proximity to the membrane surface. Nevertheless, the degree of biological uncertainty in this system is relatively high since our model does not account for different types of receptors [1,12,16] and the possibility that multiple fluorophores can reside in more than one location on the donor. Rather than increasing the complexity of our model, we present a straightforward mathematical and experimental framework using various combinations of donor–acceptor probes, in order to estimate a range of binding distances.

Experiments are performed in a plasma membrane vesicle system in which transmembrane receptors reside intact, but the interior of the vesicles is devoid of cytoplasmic structures. This provides a more optically transparent medium for fluorescence measurements but preserves the native environment of the receptor. A ligand recognized by the receptor is labeled with donor and the ligand is allowed to bind. Hydrophobic acceptor molecules are titrated to the vesicle samples and these partition into the membrane. As the concentration of acceptor in the membrane increases, there is a corresponding decrease in the quantum yield of the donor. The relative decrease is a function of the surface density of acceptors and can be described by a single exponential. The decay constant for the exponential, in turn, is a function of the distance between the donor and the acceptors.

Thus, a distance measurement can be obtained from a simple experiment monitoring the change of donor fluorescence over a range of titration of acceptors to the plasma membrane vesicle system.

In this work, energy transfer measurements with dansyl-labeled mal-BSA and two amphipathic acceptors, HAE and ORB, place the bound mal-BSA molecules at about 47–58 Å from the membrane surface. HAE is an anionic membrane probe, while ORB is a cationic membrane probe. Obtaining similar distance measurements with both acceptor systems supports the validity of using an orientation factor of 2/3 and, in addition, suggests the absence of any charge–charge aggregation of probes in the membrane [18].

Mal-BSA was labeled at multiple sites by dansyl; thus, the distances obtained represent an average location for the various labeling sites (approximate center of the BSA molecule). This average is heavily weighted by the donors nearer to the surface so it does not represent the approximate center of the molecule. More specific labeling was achieved with fluorescein maleimide. This fluorescein derivative specifically labels thiol groups. The sole free cysteine group in BSA lies at position 34 on the N-terminal end of the ellipsoidal BSA molecule, measured to be 140 × 41 Å by hydrodynamic and electron microscopic methods [26]. Interestingly, measurements conducted with the monolabeled fluorescein mal-BSA failed to exhibit transfer, implying that the fluorescein-labeled residue lay too far from the membrane surface to experience resonance energy transfer with the acceptor. The orientation of mal-BSA in the binding site must then be such that the N terminus is located too far from the membrane surface to experience transfer.

These optical techniques are broadly applicable to any receptor–ligand system, as long as the ligand can be fluorescently tagged. Recently, two types of class A receptors have been identified, types I and II, which are similar in structure, a rigid stalk, except for the absence of a cysteine-rich domain in the type II receptor [2,25,32]. In a rigid stalk model the distance results obtained here place the binding site in the α-helical coiled-coil domain of the receptor. Studies on this class of receptor suggest the presence of multiple binding sites with differing specificities [3,11,13,17,28]. Previous binding studies have focused on the collagen-like domain of the receptor. Traditional mutation experiments are difficult to perform in the α-helical coiled-coil domain since this region is required for structural integrity of the receptor. Our experiments indicate that a binding site may reside in this region. In recent years a class B scavenger receptor has been identified [1,12,16]. Since mal-BSA is recognized by two receptor types, our measurements yield an average distance from the plasma membrane surface for the ligand. This could be refined to a precise distance in a single receptor system—such as membrane vesicles from transfected cells expressing only one of the receptors. The preparation of plasma membrane vesicles can be applied to any cell type and has the distinct advantage of allowing the study of transmembrane proteins *in situ*. By comparing the distance information to the predicted structure of the protein, one can identify a position for the binding site which can then be compared to the primary structure to extract binding sequence information.

FRET for the determination of binding site location relative to the membrane surface is best suited for study of proteins with a somewhat rigid structure. Extremely flexible proteins could yield ambiguous results since they are likely to assume a wide range of conformations in the course of measurement. Alternatively, the acceptor(s) could be positioned at various sites on the receptor rather than in the plasma membrane and the distance determinations of the donor from these acceptors correlated, to construct a more precise structural model.

Probing of receptor–ligand interactions by this application of FRET offers an attractive alternative to traditional methods for structure determination which are not well suited for transmembrane protein studies. FRET has the distinct advantage of allowing observation of the wildtype transmembrane receptor in its native environment. Distance/interaction information derived by FRET can be applied to locate potential binding regions, which can be further investigated by biochemical methods, or isolated for higher resolution structural determinations. FRET is a valuable addition to the repertory of techniques currently available for the study of receptor structure and function.

ACKNOWLEDGMENTS

The authors wish to thank Drs. Chung Ho Sun, Bill Wright, and Kenneth Longmuir for many helpful discussions. Thanks go also to our lab associates Pam Templin, Kalvin Yu, Dr. Tatiana Krasieva, Glenn Profeta, and Jeff Andrews for their assistance and support in this project. This work was supported by Office of Naval Research Grant N00014-91-C-0134, National Institutes of Health LAMMP Resource Facility P41RR01192, Department of Energy Grant DE-FG03-91ER61227, and Training Program in Carcinogenesis Grant 5 T32CA09054

REFERENCES

1. A. L. Acton, P. E. Scherer, H. F. Lodish, and M. Kreiger (1994) *JBC* **269**(33), 21003–21009.
2. S. Acton, D. Resnick, M. Freeman, Y. Ekkel, J. Ashkenas, and M. Krieger (1993) *JBC* **268**(5), 3530–3537.
3. H. Arai, T. Kita, M. Yokode, S. Narumiya, and C. Kawai (1989) *Biochem. Biophys. Res. Commun.* **159**(3), 1375–1382.
4. B. Baird and D. Holowka (1988) *Structural Mapping of Membrane-Associated Proteins: A Case Study of the IgE-Receptor Complex*, CRC Press, New York.
5. B. Baird and D. Holowka (1985) *Biochemistry* **24**, 6252–6259.
6. M. Brown and J. L. Goldstein (1983) *Annu. Rev. Biochem.* **52**, 223–261.
7. P. G. Butler and B. S. Hartley (1972) *Methods Enzymol.* **25**, 191–199.
8. L. Cantley Jr. and G. G. Hammes (1975) *Biochemistry* **14**(13), 2976–2981.
9. R. E. Dale, J. Eisinger, and W. E. Blumberg (1979) *Biophys. J.* **26**, 161–194.
10. T. Dewey and G. Hammes (1980) *Biophys. Soc.* **32**, 1023–1035.
11. H. A. Dresel, E. Freidrich, D. P. Via, H. Sinn, R. Ziegler, and G. Schetter (1987) *EMBO J.* **6**(2), 319–326.
12. G. Endemann, L. W. Stanton, K. S. Madden, C. M. Bryant, R. T. White, and A. A. Protter (1993) *JBC* **268**(16), 11811–11816.
13. M. Freeman, Y. Ekkel, L. Rohrer, M. Penman, N. J. Freedman, G. M. Chisholm, and M. Krieger (1991) *Proc. Natl. Acad. Sci. USA* **88**, 4931–4935.
14. B. Fung and L. Stryer (1978) *Biochemistry* **17**(24), 5241–5248.
15. J. L. Goldstein, Y. K. Ho, K. Basu, and M. S. Brown (1979) *Proc. Natl. Acad. Sci. USA* **76**(1), 333–337.
16. D. E. Greenwalt, R. H. Lipsky, C. F. Ockenhouse, H. Ikeda, N. N. Tandon, and G. A. Jamieson (1992) *Blood* **80**(5), 1105–1115.
17. M. E. Haberland, C. S. Tannenbaum, R. E. Williams, D. O. Adams, and T. A. Hamilton (1989) *J. Immunol.* **142**(3), 855–862.
18. G. G. Hammes (1981) in C. Frieden and L. W. Nichol (Eds.), *Protein-Protein Interactions*, John Wiley and Sons, New York, pp. 257–287.
19. R. Haugland (1992) *Molecular Probes: Handbook of Fluorescent Probes and Research Chemicals*, Molecular Probes, Eugene, OR.
20. D. Holowka and B. Baird (1983) *Biochemistry* **22**, 3466–3474.
21. D. Holowka and B. Baird (1983) *Biochemistry* **22**, 3466–3474.
22. E. J. Husten, C. T. Esmon, and A. E. Johnson (1987) *JBC* **262**(27), 12953–12961.
23. D. Johnson and J. Nuss (1994) *Biochemistry* **33**(31), 9070–9077.
24. D. A. Johnson, R. Cushman, and R. Malekzade (1990) *JBC* **265**(13), 7360–7368.
25. T. Kodama, M. Freeman, L. Rohrer, J. Zabrecky, P. Matsudaira, and M. Krieger (1990) *Nature* **343**, 533–535.
26. U. Kragh-Hansen (1990) *Danish Med. Bull.* **37**(1), 57–81.
27. K. J. Longmuir, O. C. Martin, and R. E. Pagano (1985) *Chem. Phys. Lipids* **36**, 197–207.
28. E. Ottnad, D. P. Via, J. Frubis, H. Sinn, E. Friedrich, R. Ziegler, and H. A. Drese (1992) *Biochem. J.* **281**, 745–751.
29. J. Pierce and C. H. Suelter (1977) *Anal. Biochem.* **82**, 478–480.
30. S. Pin, C. A. Royer, E. Gratton, B. Alpert, and G. Weber (1990) *Biochemistry* **29**, 9194–9202.
31. E. J. Robertson (1987) *Teratocarcinomas and Embryonic Stem Cells*, IRL Press, Oxford, England.
32. L. Rohrer, M. Freeman, T. Kodama, M. Penman, and M. Krieger (1990) *Nature* **43**, 570–572.
33. B. Snyder and E. Freire (1982) *Biophys. J.* **40**, 137–148.
34. D. Steinberg, S. Parthasarathy, T. E. Carew, J. C. Khoo, and J. L. Witztum (1989) *N. Engl. J. Med.* **320**(14), 915–924.
35. C. Valenzuela, A. Dowding, H. Arias, and D. Johnson (1994) *Biochemistry* **33**, 6586–6594.
36. C. F. Valenzuela, P. Weign, J. Yguerabide, and D. A. Johnson (1994) *Biophys. J.* **66**, 674–682.
37. P. K. Wolber and B. S. Hudson (1979) *Biophys. J.* **28**, 197–210.
38. Y. Zheng, B. Shopes, D. Holowka, and B. Baird (1991) *Biochemistry* **30**, 9125–9132.